Implemented Wavelet Packet Tree based Denoising Algorithm in Bus Signals of a Wearable Sensorarray

Schimmack, Manuel; Nguyen, Susi; Mercorelli, Paolo

Published in:
Journal of Physics: Conference Series

DOI:
10.1088/1742-6596/659/1/012021

Publication date:
2015

Document Version
Publisher's PDF, also known as Version of record

Implemented Wavelet Packet Tree based Denoising Algorithm in Bus Signals of a Wearable Sensorarray

Journal of Physics: Conference Series **659** (2015) 012021 doi:10.1088/1742-6596/659/1/012021

Implemented Wavelet Packet Tree based Denoising Algorithm in Bus Signals of a Wearable Sensorarray

M. Schimmack, S. Nguyen, P. Mercorelli
Institute of Product and Process Innovation
Leuphana University of Lueneburg
Volgershall 1, D-21339 Lueneburg, Germany

E-mail: [schimmack, mercorelli]@uni.leuphana.de

Abstract. This paper introduces a thermosensing embedded system with a sensor bus that uses wavelets for the purposes of noise location and denoising. From the principle of the filter bank the measured signal is separated in two bands, low and high frequency. The proposed algorithm identifies the defined noise in these two bands. With the Wavelet Packet Transform as a method of Discrete Wavelet Transform, it is able to decompose and reconstruct bus input signals of a sensor network. Using a seminorm, the noise of a sequence can be detected and located, so that the wavelet basis can be rearranged. This particularly allows for elimination of any incoherent parts that make up unavoidable measuring noise of bus signals. The proposed method was built based on wavelet algorithms from the WaveLab 850 library of the Stanford University (USA). This work gives an insight to the workings of Wavelet Transformation.

1. Introduction

Over the past decades, Wavelets have become another important tool that has established its industrial use in fields such as signal analysis, data compression and also noise reduction. They are mathematical functions, that essentially present an extension to the already primarily used Fourier Transform, however, with the properties to have not only time-based but also frequency-based results. The Fourier Transform is helpful for trigonometric functions but lacks in performance with other types. One reason to prefer the Wavelet Transform over the traditional Fourier Transform is its better resolution to give accurate information about frequencies at certain times, and it is also more suited in approximation of signals with discontinuities and sharp spikes.

The proposed wearable application can be used for thermosensing of the changes and fluctuations in temperature of the extremity surfaces of a patient. In a human body, the body temperature stays constant as long as its energy gain and energy loss are equal. If this condition is not met, the temperature is able to fluctuate, resulting in either heat generation or loss. Thereby, the body temperature can be increased by parameters such as metabolism and emotions, food or physical activity. Another important impact is conducted through the environment, where a human being is able to experience heat exchanges through the skin. One can differentiate into the body core temperature and the skin temperature, the latter being highly dependent on the environmental conditions. As humans are warm-blooded mammals, the body core temperature is maintained constant at a range of $36.8 - 37.7°C$. In contrast, the extremities and skin are the ones that adapt to outer changes to protect the body core.

A thermoregulation process is performed by the body with help of the hypothalamus, where central sensors for the body core temperature are located. It also receives information about the skin temperature through thermal receptors under the skin, and also brain and spinal cord. When the body temperature strays from the set point its supposed to be, the hypothalamus is able to adjust the temperature through reflexes like sweating, shivering or changes in skin blood flow. With this, the body is able to regulate its own temperature. To measure the changes of the skin temperature, a temperature sensor network, which is implemented in a textile substrate is used. These sensors are connected to each other over conductive polymer-metal composite fibers to a sensor array and communicate over a bus system. Conductive polymer-metal composite fibers are the fundamental core for wearable technology and an integral part of smart textiles. There is a wide field of applications both in use and in development, which is analyzed in [1]. As traditional utilization, the yarn is used as a textile electrode as well as a transmission line for monitoring of physiological parameters as exhibited in [2]. Combined with an analyzing algorithm the fibers have been presented in context of a wearable orthosis-system after a bone fracture in [3] for monitoring during the predictive rehabilitation.

One of the pionier contributions of wavelet-denoising approach and thresholding can be found in [4] and also in [5]. Naturally measurement noises and disturbances occur during application, thus an adaptive filter is needed. Therefore a wavelet based denoising algorithm is built based on the WaveLab 850 of Stanford University [6], using the Haar wavelet family to accurately represent the form of a rectangular bus signal.

2. Wavelet Decomposition Method

The Haar Wavelet has a simple square wave structure, making it preferably used in analyzing compact discrete signals. For Wavelet Transformation, a wavelet function and a scaling function are needed. The Haar Wavelet's basis wavelet function, also known as the mother wavelet, can be described as follows

$$\psi_{(d,b,k)}(t) = \psi_b(2^d t - n), \tag{1}$$

with a support of size 2^{-d} of the Nyquist frequency and the indices (d, b, k). Herein, d is set as a scale index describing the tree level, b as a phase parameter for the frequency shift and k as a time related parameter indicating the shift in time. Also the mother wavelet's structure is shown by the dependencies

$$\psi(t) = \begin{cases} 1 & \text{if } 0 \leq t < \frac{1}{2} \\ -1 & \text{if } \frac{1}{2} \leq t < 1 \\ 0 & \text{for all other } t \end{cases} \tag{2}$$

As a decomposition method, this paper uses the Wavelet Packet Transform which belongs to the method of Discrete Wavelet Transform and creates a complete wavelet basis decomposition tree. Using this tree structure, the input signal that is going to be analyzed, will be disassembled into subspaces that hold either high frequency or low frequency sequences. Subsequently this procedure is done for different levels of the tree, repeating the filtration of Wavelet Father into two Wavelet Children, one of high and one of low frequency. Such a process enables the separation of the noise and the actual signal. The weighted coefficients $wp(d, b, k)$ are calculated in more detail as follows

$$wp_{(d,b,k)} = \int_I f(t)\psi^h_{(d,b,k)}(t)d(t). \tag{3}$$

For $b = 0$ it is possible to define the following coefficients

$$s_{(d,0,k)} = \int_I f(t)\psi^h_{(d,0,k)}(t)d(t), \tag{4}$$

where $f(t)$ is the required signal, I is the considered time interval and $\psi^h_{(d,0,k)}(t)$ is the well known mother function of a Haars wavelet [7]. To conclude

$$f(t) = \sum_k s_{(d,k)} \psi^h_{(d,0,k)}(t) + \sum_b \sum_k wp_{(d,b,k)} \psi^h_{(d,b,k)}, \tag{5}$$

where $s_{(d,k)} = wp_{(d,0,k)}$. It is shown that there are just two independent parameters and that parameter d characterizes the level of the tree. The wavelet packets under consideration are derived from the Haar mother wavelet. The Haar functions are identified using the parameter tuple, (d, b, k), here $d = 1$ represents the highest degree of refinement with respect to time. Fig. 1 shows the corresponding tree with the wavelet coefficients, described by $wp_{(d,b,k)}$. It represents the contribution of each of the wavelets to the signal based on n samples. The notation $wp_{(1,0,0\ldots\frac{n}{2}-1)}$ denotes the coefficients on the first level on the left with time shifts 0 through $\frac{n}{2} - 1$.

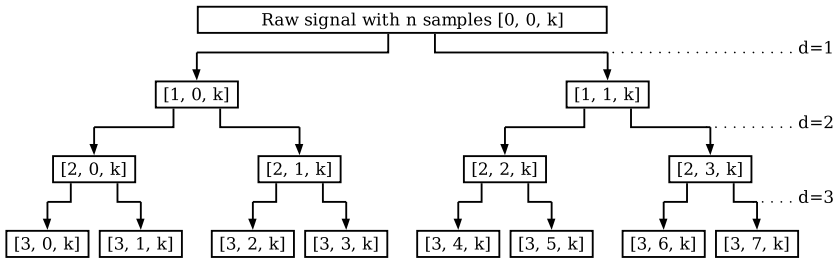

Figure 1. The Wavelet coefficients arranged in a tree-like structure based on WaveLab Version 850 with different scale index d

3. Wavelet Denoising Method using an axiomatic Seminorm

In order to detect the noise $e(t)$ in a measured signal $y(t)$ characterization through a possible definition is required. For the definition of the noise in a bus signal a seminorm will be used.

Definition 1

$$p(\mathbf{V}) = \Big|\sum\nolimits_{k=0}^{2^{D-d}} \{wp_{(d,b,k)}\}\Big|, \tag{6}$$

where $\mathbf{V}$ *represents a vectorial field and in general* $p : \mathbf{V} \to \mathbb{R}^+$. □

Function $p(\mathbf{V})$ satisfies the positivity, absolute homogeneity and subadditivity properties, but it does not satisfy the separation property. In more detail, if $p(\mathbf{V}) = 0$, it does not necessarily imply that sequence (vector) $\mathbf{V} = 0$. A possible definition of a noise is proposed as follows.

Definition 2 *Given an observed sequence*

$$y(t) = x(t) + e(t). \tag{7}$$

Let $e(t)$ *be defined as the incoherent part of the sequence* $y(t)$ *at every level* d *of the packet tree as shown below*

$$e(t) = \sum_{(\mathbf{d}_{ml},\mathbf{b}_{ml})} \sum_{k=0}^{2^{D-d}} wp_{(\mathbf{d}_{ml},\mathbf{b}_{ml},k)} \psi_{(\mathbf{d}_{ml},\mathbf{b}_{ml},k)}(t) + \sum_{(\mathbf{d}_{mh},\mathbf{b}_{mh})} \sum_{k=0}^{2^{D-d}} wp_{(\mathbf{d}_{mh},\mathbf{b}_{mh},k)} \psi_{(\mathbf{d}_{mh},\mathbf{b}_{mh},k)}(t), \tag{8}$$

where if a specified length n (dyadic length) is considered to determine the height of the wavelet tree: $D = \log_2(n)$. *For characterization of the selected wavelets, the whole decomposition tree starting from level d=1 is split in half, dividing the tree into a low frequency domain on the left and a high frequency domain on the right. This is in analogy to wavelets working as a filter bank, as the tree is separated into two bands, low and high frequency. Here, the selected wavelets are defined by* $(\mathbf{d}_{ml}, \mathbf{b}_{ml})$ *for the low frequency and* $(\mathbf{d}_{mh}, \mathbf{b}_{mh})$ *for the high frequency subspaces indices such that*

$$\{(\mathbf{d}_{ml}, \mathbf{b}_{ml})\} = arg\Big(\min_{(d,b)} |\sum_{k=0}^{2^{D-d}} \{wp_{(d,b,k)}\}|) : \{0 \leq k \leq 2^{D-d}, 0 \leq b \leq 2^{d-1} - 1, \forall d \in \mathbb{N}\}\Big), \tag{9}$$

$$\{(\mathbf{d}_{mh}, \mathbf{b}_{mh})\} = arg\Big(\min_{(d,b)} |\sum_{k=0}^{2^{D-d}} \{wp_{(d,b,k)}\}|) : \{0 \leq k \leq 2^{D-d}, 2^{d-1} \leq b \leq 2^{d} - 1, \forall d \in \mathbb{N}\}\Big). \tag{10}$$

□

In effect, the definition of the noise looks for the subspace characterized by the minimum of the components in both the low and the high frequency wavelet domain. Defenition 2 is used to sort the wavelet basis, which can illuminate the difference between the coherent and incoherent part of the sequence.

3.1. Description of the algorithm

The proposed algorithm works in the following way, starting from the second level of the wavelet packet tree (d=2). With the defined axiomatic seminorm, the minima of both frequency domains are calculated, resulting in one minimum subspace for the low and one for the high frequency domain. Once the minima at level d=2 are calculated with respect to b, the seminorm for each of their two children are calculated at level d=3 (d+1). Now when comparing the seminorm values for the minimum of a father to his descending children, if the sum of the children is less than that of the father, the noise is localized with the children. Otherwise the noise if located with the father subspace. In case of the noise being located with the children, both the subspaces are compared again, and the one with a smaller seminorm calculation represents the noise. This process is done for both high and low frequency domain, specifying one minimum subspace in each domain where the noise is located. For denoised reconstruction, those subspaces that are determined to represent noise, are left out. This way, the algorithm subsequently searches for a minimum down until the end of the tree.

3.2. Signal cleaning procedure

Given the sampled signal

- **Step 1**: Specify dyadic length, n, in order to determine the height of the wavelet tree: $D = \log_2(n)$.
- **Step 2**: Construct the wavelet coefficient tree $wp_{(d,b,k)}$ for every $d \geq 0$ and for every k.
- **Step 3a**: For the time-frequency intervals such that $b = 0, 1, ...2^{d-1} - 1$ with $d > 1$, calculate the absolute value of the $\sum_k$ for the low frequency intervals of the tree, that is, $W_{ml}sum(d, b) = |\sum_k W(d, b)|$.

- **Step 3b**: For all time-frequency intervals such that $b = 2^{d-1}, 2^{d-1}+1, ...2^d - 1$ with $d > 1$, calculate the absolute value of the $\sum_k$ for the high frequency intervals of the tree, that is, $W_{mh}sum(d,b) = |\sum_k W(d,b)|$.
- **Step 4a**: For every "wavelet father" of the low frequency domain $W_{ml}(d,b)$ at the node (d,b) with $b = 0, 1, ...2^{d-1} - 1$, calculate its left child at the node $(d+1, bLeft)$ and its right child $(d+1, bRight)$. Then, calculate the absolute value of the sum with respect to k and denote them as

$$W_{ml}sumChildLeft = \big|\sum\nolimits_k W_{ml}sum(d, bLeft)\big| \tag{11}$$

and

$$W_{ml}sumChildRight = \big|\sum\nolimits_k W_{ml}sum(d, bRight)\big|. \tag{12}$$

While $(d < D)$
For $b = 0 : 2^{d-1} - 1$
Case

$$W_{ml}sum(d,b) \leq W_{ml}sumChildLeft + W_{ml}sumChildRight :$$
$$\mathbf{W}_{ml}b(d_{ml}, b_{ml}) = arg\big(\min_{(d,b)} W_{ml}sum(d,b)\big)$$

Case

$$W_{ml}sumChildLeft \leq W_{ml}sumChildRight :$$
$$\mathbf{W}_{ml}b(d_{ml}, b_{ml}) = arg\big(\min_{(d,b)} W_{ml}sumChildLeft\big)$$

Case

$$W_{ml}sumChildRight \leq W_{ml}sumChildLeft :$$
$$\mathbf{W}_{ml}b(d_{ml}, b_{ml}) = arg\big(\min_{(d,b)} W_{ml}sumChildRight\big)$$

End b loop

- **Step 4b**: In the same pattern as in the previous step, the procedure of noise location is done for the high frequency domain. For every "wavelet father" of the high frequency domain $W_{mh}(d,b)$ at the node (d,b) with $b = 2^{d-1}, 2^{d-1}+1, ...2^d - 1$, calculate its left child at the node $(d+1, bLeft)$ and its right child $(d+1, bRight)$. Then, calculate the absolute value of the sum with respect to k and denote them as

$$W_{mh}sumChildLeft = \big|\sum\nolimits_k W_{mh}sum(d, bLeft)\big| \tag{13}$$

and

$$W_{mh}sumChildRight = \big|\sum\nolimits_k W_{mh}sum(d, bRight)\big|. \tag{14}$$

For $b = 2^{d-1} : 2^d - 1$.
Case

$$W_{mh}sum(d,b) \leq W_{mh}sumChildLeft + W_{mh}sumChildRight :$$
$$\mathbf{W}_{mh}b(d_{mh}, b_{mh}) = arg\big(\min_{(d,b)} W_{mh}sum(d,b)\big)$$

Case

$$W_{ml}sumChildLeft \leq W_{mh}sumChildRight :$$
$$\mathbf{W}_{mh}b(d_{mh}, b_{mh}) = arg\big(\min_{(d,b)} W_{mh}sumChildLeft\big)$$

Case

$$W_{ml}sumChildRight \leq W_{mh}sumChildLeft$$
$$\mathbf{W}_{mh}b(d_{mh}, b_{mh}) = arg\big(\min_{(d,b)} W_{mh}sumChildRight\big)$$

End b loop

- **Step 5**: Reconstruct the noise

$$e(t) = \sum_{(\mathbf{d}_{ml},\mathbf{b}_{ml})} \sum_{k=0}^{2^{D-d}} wp_{(\mathbf{d}_{ml},\mathbf{b}_{ml},k)}\psi_{(\mathbf{d}_{ml},\mathbf{b}_{ml},k)}(t) + \sum_{(\mathbf{d}_{mh},\mathbf{b}_{mh})} \sum_{k=0}^{2^{D-d}} wp_{(\mathbf{d}_{mh},\mathbf{b}_{mh},k)}\psi_{(\mathbf{d}_{mh},\mathbf{b}_{mh},k)}(t) \tag{15}$$

and reconstruct the denoised signal

$$y_d(t) = y(t) - e(t). \tag{16}$$

4. Methodology and Embedded System

4.1. Sensor Bus

The DS18S20 digital thermosensor provides with a modification 12-bit Celsius temperature measurements and has an alarm function with nonvolatile user-programmable upper and lower trigger points. The sensor communicates over a 1-Wire bus which used one data line, power line and ground for communication with a embedded system. Fig. 2 shows that each sensor has a unique 64-bit serial code, which allows multiple sensors to function on the same 1-Wire bus. Thus, it is possible to use the embedded system to control many sensors distributed over a large area.

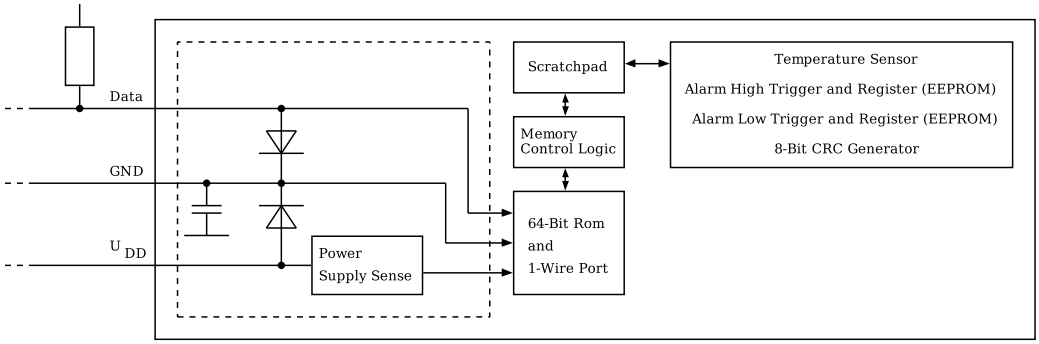

Figure 2. General block diagram of the high-precision 1-Wire digital thermosensor and its components.

4.2. Embedded System

A portable Linux based embedded system, which is depicted in Fig. 3 with the corresponding components, works like a signal processing module. The sensorarray them self is implemented in a textile substratum and connected over the 1-Wire bus to the sensorarray. The embedded system based on the Broadcom BCM2836 system on a chip (SoC) and has a quad-core ARM Cortex-A7 central processing unit (CPU) with a VideoCore IV dual-core graphics processing unit (GPU). The used Linux kernel for the operating system based on the ARM hard-float (armhf) Debian architecture and the proposed algorithm works with GNU Octave.

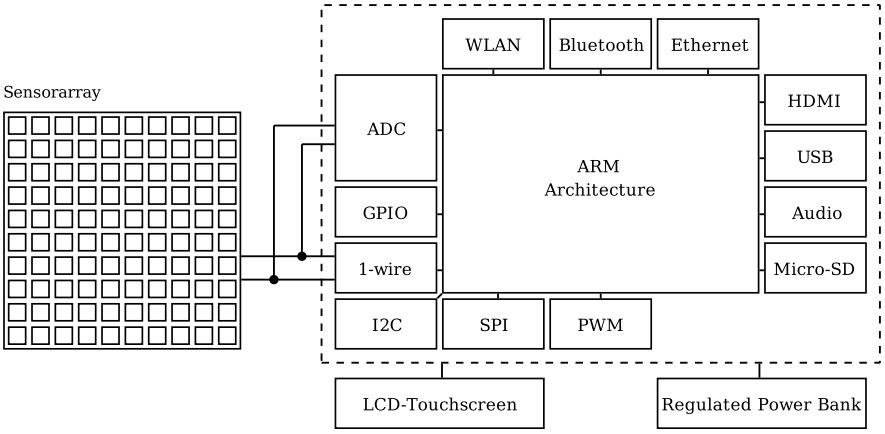

Figure 3. General block diagram of the measurement system with the Linux based embedded system.

5. Validation

To showcase the effectiveness of the algorithm, the denoising performance is observed for a synthetically generated noisy square wave signal, which can be analogously compared to that of a bus signal. With this, Fig. 4 shows the result of the algorithm for the reconstruction with the global minimum of the frequency domains as the noise component. On the other hand, Fig. 5 shows the result of the algorith for the reconstruction with both the minimum value of the low and minimum value of the high frequency domain as noise components. It is shown graphically, how the method in Fig. 5 is superior in suppressing noise, as the amplitude of the reconstruction is visibly lower than in Fig. 4. This proves that the here proposed algorithm method is indeed more effective in denoising than a method of only eliminating the global minimum of the frequency domains. Fig. 6 a shows the free upper limb with the implemented sensors in the textile substrate and a general visualization of the temperature surface [8]. Therefor the char of temperature values were transformed into the RGB-colours as

$$\lambda = \begin{cases} (0, k, 255), & k < 256 \\ (0, 255, 512 - k), & 256 \leq k < 768 \\ (255, 1024 - k, 0), & 768 \leq k < 1024 \end{cases} \tag{17}$$

The value k based on the interval $[0, 1024[$ to $\mathbb{R}$ and λ presents the colour of the RGB-sequence with $R \in [0, 255], G \in [0, 255], B \in [0, 255]$. The nearest neighbor interpolation represents in Fig. 6b a general algorithm for the visualization of the sensorarray values with

$$f(x, y) = \begin{cases} f(Q_{11}), x < x_2 - \frac{\Delta x}{2}, y < y_2 - \frac{\Delta y}{2} \\ f(Q_{12}), x > x_2 - \frac{\Delta x}{2}, y < y_2 - \frac{\Delta y}{2} \\ f(Q_{21}), x < x_2 - \frac{\Delta x}{2}, y > y_2 - \frac{\Delta y}{2} \\ f(Q_{22}), x > x_2 - \frac{\Delta x}{2}, y > y_2 - \frac{\Delta y}{2} \end{cases} \tag{18}$$

was used. Fig. 7 shows the graphical representation of the forearm with a) the bilinear interpolation like

$$\begin{aligned} f(x, y) \approx & \frac{f(Q_{11})}{(x_2 - x_1)(y_2 - y_1)}(x_2 - x)(y_2 - y) + \frac{f(Q_2 1}{(x_2 - x_1)(y_2 - y_1)}(x - x_1)(y_2 - y) \\ & + \frac{f(Q_1 2}{(x_2 - x_1)(y_2 - y_1)}(x_2 - x)(y - y_1) + \frac{f(Q_2 2}{(x_2 - x_1)(y_2 - y_1)}(x - x_1)(y - y_1) \end{aligned} \tag{19}$$

and b) a bicubic spline-interpolation of the sensorarray values was used.

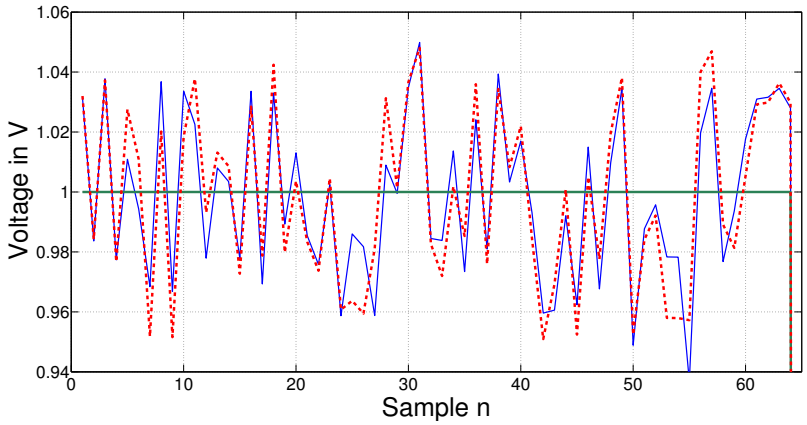

Figure 4. Graphical representation of the reconstruction without the global minimum of the frequency domains.

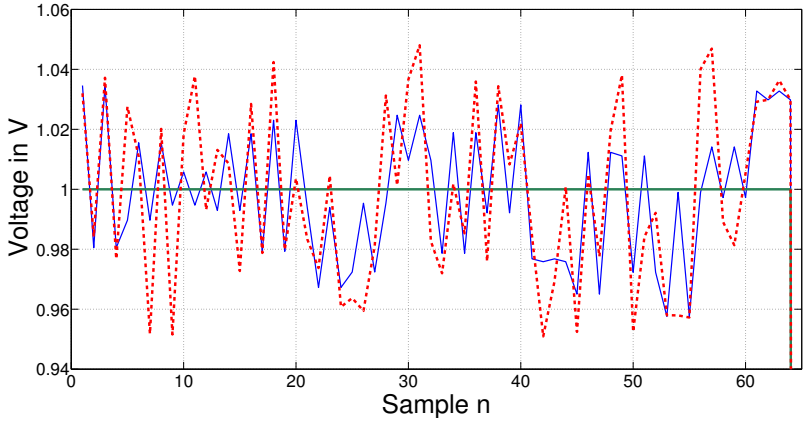

Figure 5. Graphical representation the reconstruction without both minimum values of the low and the high frequency domain.

6. Conclusion

The paper analyzes the properties of denoising 1-Wire bus signals of a temperature sensorarray for longterm monitoring of the skin surface based on Haar wavelets. With the Wavelet Packet Transform as a method of Discrete Wavelet Transform, it was able to decompose and reconstruct bus input signals of a sensor network. Using a seminorm, the noise of a sequence can be detected and located, so that the wavelet basis can be rearranged. In fact, the wavelets reduces the effect of the noise which can be applied directly without using model noise. This particularly allows for elimination of any incoherent parts that make up unavoidable measuring noise of bus signals. The proposed method was built based on wavelet algorithms from the WaveLab 850 library of the Stanford University (USA). This work gives an insight to the workings of Wavelet Tranformation. The results show the effectiveness of the proposed technique. Even though the

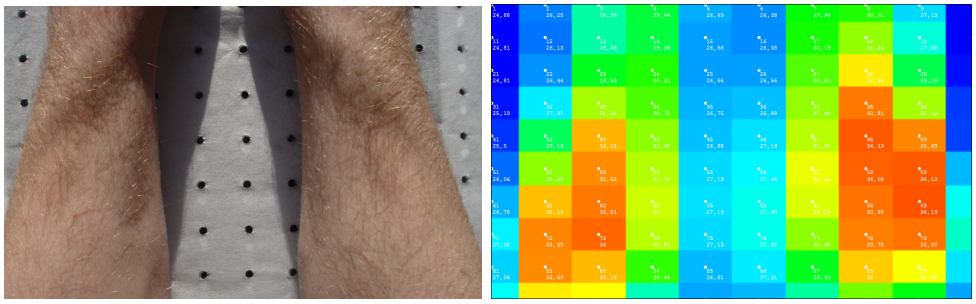

Figure 6. Free upper limb with the implemented sensors in the textile substrate and a general visualization of the temperature surface.

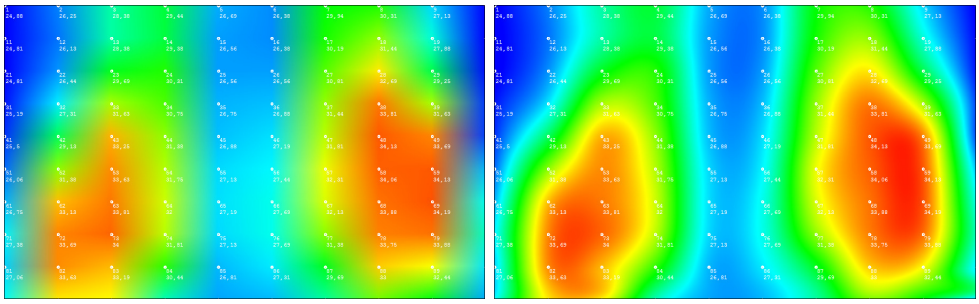

Figure 7. Graphical representation of the forearm with a) the bilinear interpolation and b) the bicubic spline-interpolation of the sensorarray values.

obtained results are quite general, results using GNU Octave and MATLAB® considering the experimental setup are shown and commented.

References

[1] A. Pantelopoulos and N. G. Bourbakis. A survey on wearable sensor-based systems for health monitoring and prognosis. *IEEE Transaction on Systems, Man, and Cybernetics Part C: Application and Review*, 40(1):1–12, 2010.

[2] N. Noury, A. Dittmar, C. Corroy, R. Baghai, J.L. Weber, D. Blanc, F. Klefstat, A. Blinovska, S. Vaysse, and B. Comet. A smart cloth for ambulatory telemonitoring of physiological parameters and activity: the vtamn project. In *IEEE HEALTHCOM - Proceedings of the 6th International Workshop on Enterprise Networking and Computing in Healthcare Industry*, pages 155–160, Japan, 2004.

[3] M. Schimmack, A. Hand, P. Mercorelli, and A. Georgiadis. Using a seminorm for wavelet denoising of sEMG signals for monitoring during rehabilitation with embedded orthosis system. In *IEEE MeMeA - International Symposium on Medical Measurements and Applications*, Italy, 2015.

[4] D. L. Donoho. Denoising and soft thresholding. *IEEE Transactions on Information Theory*, 41(3):613–627, 1995.

[5] S. Neville and N. Dimopoulos. Wavelet denoising of coarsely quantized signals. *IEEE Transactions on Instrumentation and Measurement*, 55(3):892–901, 2006.

[6] J. Buckheit, S. Chen, D. Donoho, I. Johnstone, and J. Scargle. About wavelab. *Handbook of WaveLab Version .850 by Standford University and NASA-Ames Research Center*, pages 1–37, 2005.

[7] P. Mercorelli and A. Frick. *Noise Level Estimation Using Haar Wavelet Packet Trees for Sensor Robust Outlier Detection*. Series: Lecture Note in Computer Sciences, Springer-Verlag publishers, 2006.

[8] M. Schimmack, R. Sukhikh, A. Georgiadis, and C. H. Siemsen. Drahtloses und bildgebendes Multi-Sensorsystem integriert in eine Handgelenksorthese für ein nichtinvasives Langzeitmonitoring. *Sensoren und Messsysteme*, 44(3):603–609, 2012.